

PT-SCOTCH: A tool for efficient parallel graph ordering

C. Chevalier^{a*}, F. Pellegrini^b

^aLaBRI & Project ScAlApplix of INRIA Futurs
351, cours de la Libération, 33400 Talence, France

^bENSEIRB, LaBRI & Project ScAlApplix of INRIA Futurs
351, cours de la Libération, 33400 Talence, France
{cchevali|pelegrin}@labri.fr

The parallel ordering of large graphs is a difficult problem, because on the one hand minimum degree algorithms do not parallelize well, and on the other hand the obtainment of high quality orderings with the nested dissection algorithm requires efficient graph bipartitioning heuristics, the best sequential implementations of which are also hard to parallelize. This paper presents a set of algorithms, implemented in the PT-SCOTCH software package, which allows one to order large graphs in parallel, yielding orderings the quality of which is only slightly worse than the one of state-of-the-art sequential algorithms. Our implementation uses the classical nested dissection approach but relies on several novel features to solve the parallel graph bipartitioning problem. Thanks to these improvements, PT-SCOTCH produces consistently better orderings than PARMETIS on large numbers of processors.

1. Introduction

Graph partitioning is an ubiquitous technique which has applications in many fields of computer science and engineering. It is mostly used to help solving domain-dependent optimization problems modeled in terms of weighted or unweighted graphs, where finding good solutions amounts to computing, eventually recursively in a divide-and-conquer framework, small vertex or edge cuts that balance evenly the weights of the graph parts.

Because there always exist large problem graphs which cannot fit in the memory of sequential computers and cost too much to partition, parallel graph partitioning tools have been developed [1,2]. The purpose of the PT-SCOTCH software (*“Parallel Threaded SCOTCH”*, an extension of the sequential SCOTCH software [3]), developed at LaBRI within the SCALAPPLIX project of INRIA Futurs, is to provide efficient parallel tools to partition graphs with sizes up to a billion vertices, distributed over a thousand processors. Because of this deliberately ambitious goal, scalability issues have to receive much attention.

One of the target applications of PT-SCOTCH within the SCALAPPLIX project is graph ordering, which is a critical problem for the efficient factorization of symmetric sparse

*This author’s work is funded by a joint PhD grant of CNRS and Région Aquitaine.

matrices, not only to reduce fill-in and factorization cost, but also to increase concurrency in the elimination tree, which is essential in order to achieve high performance when solving these linear systems on parallel architectures. We therefore focus in this paper on this specific problem, although we expect some of the algorithms presented here to be reused in the near future in the context of edge, k-way partitioning.

The two most classically-used reordering methods are minimum degree and nested dissection. The minimum degree algorithm [4] is a local heuristic which is extremely fast and very often efficient thanks to the many improvements which have been brought to it [5–7], but it is intrinsically sequential, so that attempts to derive parallel versions of it have not been successful [8], especially for distributed-memory architectures. The nested dissection method [9], on the contrary, is very suitable for parallelization, since it consists in computing a small vertex set that separates the graph into two parts, ordering the separator vertices with the highest indices available, then proceeding recursively on the two separated subgraphs until their size is smaller than a specified threshold.

This paper presents the algorithms which have been implemented in PT-SCOTCH to parallelize the nested dissection method. The distributed data structures used by PT-SCOTCH will be presented in the next section, while the algorithms that operate on them will be described in Section 3. Section 4 will show some results, and the concluding section will be devoted to discussing some on-going and future work.

2. Distributed data structures

Since PT-SCOTCH extends the graph ordering capabilities of SCOTCH in the parallel domain, it has been necessary to define parallel data structures to represent distributed graphs as well as distributed orderings.

2.1. Distributed graph

Like for centralized graphs in SCOTCH as well as in other software packages such as METIS [1], distributed graphs are classically represented in PT-SCOTCH by means of adjacency lists. Vertices are distributed across processes along with their adjacency lists and with some duplicated global data, as illustrated in Figure 1. In order to allow users to create and destroy vertices without needing any global renumbering, every process is assigned a user-defined range of global vertex indices. Range arrays are duplicated across all processes in order to allow each of them to determine the owner process of any non-local vertex by dichotomy search, whenever necessary.

Since many algorithms require that local data be attached to every vertex, and since global indices cannot be used for that purpose, all vertices owned by some process are also assigned local indices, suitable for the indexing of compact local data arrays. This local indexing is extended so as to encompass all non-local vertices which are neighbors of local vertices, which are referred to as “ghost” or “halo” vertices. Ghost vertices are numbered by ascending process number and by ascending global number, such that, when vertex data have to be exchanged between neighboring processes, these data can be agglomerated in a cache-friendly way on the sending side, by sequential in-order traversal of the data array, and be received in place in the ghost data arrays on the receiving side.

A low-level halo exchange routine is provided by PT-SCOTCH, to diffuse data borne by local vertices to the ghost copies possessed by all of their neighboring processes. This

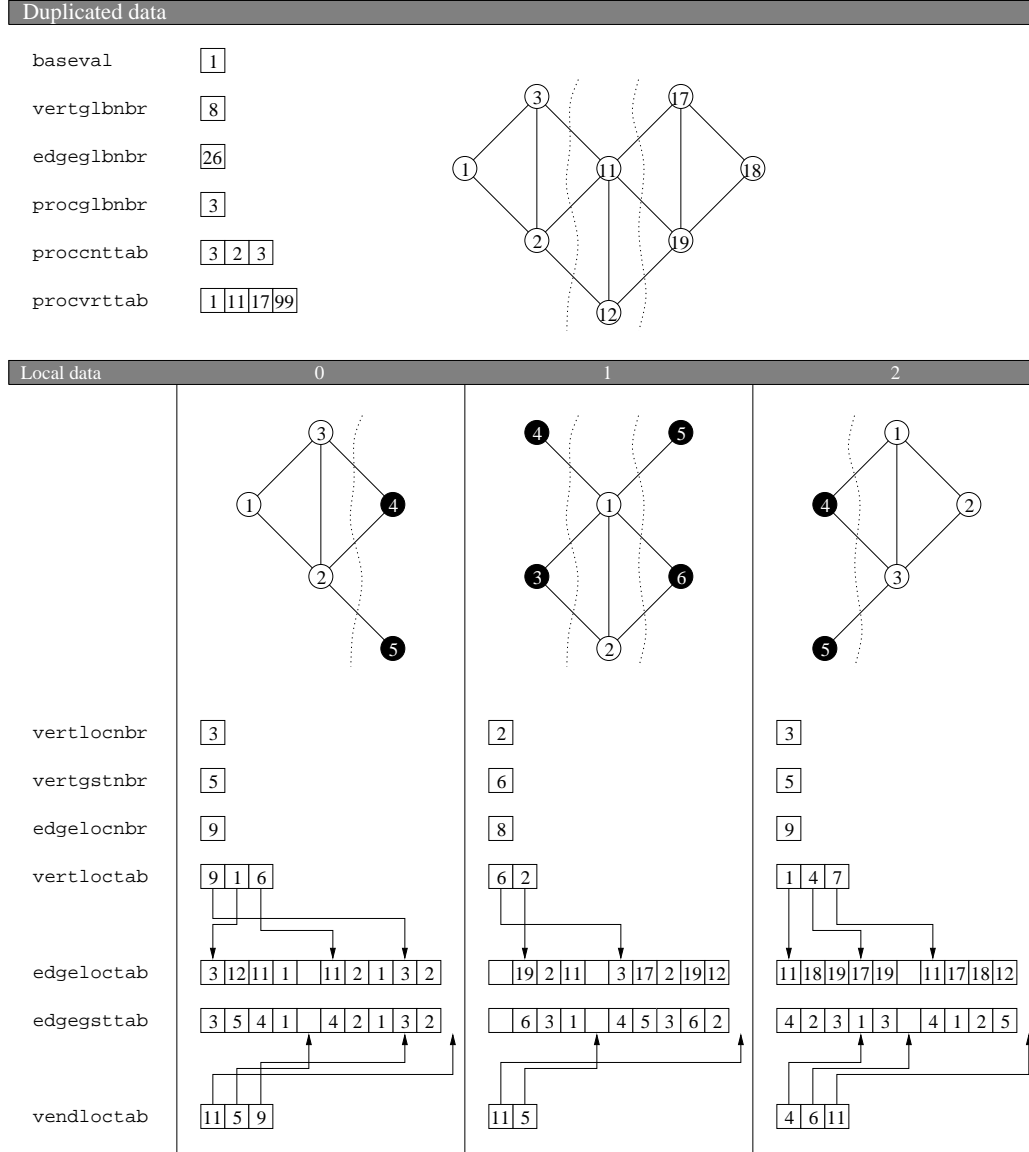


Figure 1. Data structures of a graph distributed across three processes. The global image of the graph is shown above, while the three partial subgraphs owned by the three processes are represented below. Adjacency arrays with global vertex indexes are stored in **edgelocstab** arrays, while local compact numberings of local and ghost neighbor vertices are internally available in **edgegsttab** arrays. Local vertices owned by every process are drawn in white, while ghost vertices are drawn in black. For each local vertex i located on process p , the global index of which is $(\text{procvrttab}[p] + i - \text{baseval})$, the starting index of the adjacency array of i in **edgelocstab** (global indices) or **edgegsttab** (local indices) is given by **vertloctab** $[i]$, and its after-end index by **vendloctab** $[i]$. For instance, local vertex 2 on process 1 is global vertex 12; its start index in the adjacency arrays is 2 and its after-end index is 5; it has therefore 3 neighbors, the global indices of which are 19, 2 and 11 in **edgelocstab**.

low-level routine is used by many algorithms of PT-SCOTCH, for instance to spread vertex labels of selected vertices in the induced subgraph building routine (see Section 3.1), or to share matching data in the coarse graph building routine (see Section 3.2).

Because global and local indexings coexist, two adjacency arrays are in fact maintained on every process. The first one, usually provided by the user, holds the global indices of the neighbors of any given vertex, while the second one, which is internally maintained by PT-SCOTCH, holds the local and ghost indices of the neighbors. Since only local vertices are processed by the distributed algorithms, the adjacency of ghost vertices is never stored on the processes, which guarantees the scalability of the data structure as no process will store information of a size larger than its number of local outgoing arcs.

2.2. Distributed ordering

During its execution, PT-SCOTCH builds a distributed tree structure, spreading on all of the processes onto which it is run, and the leaves of which represent fragments of the inverse permutation vector describing the computed ordering. We use inverse permutation vectors to represent orderings, rather than direct permutations, because inverse permutations can be built and stored in a fully distributed way.

Every subgraph to be reordered at some stage of the nested dissection process is only provided with the global start index, in the inverse permutation array, of the sub-ordering to compute on its vertices. If the subgraph is too small to be separated or resides on a single process, it is reordered using sequential methods, and the corresponding inverse permutation fragment is built, of a size equal to the number of vertices in the subgraph, and filled with the original global indices of the reordered subgraph vertices, in local inverse permutation order. At the end of the nested dissection process, the assembly of all of these fragments, by ascending start indices, yields the complete inverse permutation vector.

3. Algorithms for efficient parallel reordering

The parallel computation of orderings in PT-SCOTCH involves three different levels of concurrency, corresponding to three key steps of the nested dissection process: the nested dissection algorithm itself, the multi-level coarsening algorithm used to compute separators at each step of the nested dissection process, and the refinement of the obtained separators. Each of these steps is described below.

3.1. Nested dissection

As said above, the first level of concurrency relates to the parallelization of the nested dissection method itself, which is straightforward thanks to the intrinsically concurrent nature of the algorithm. Starting from the initial graph, arbitrarily distributed across p processes but preferably balanced in terms of vertices, the algorithm proceeds as illustrated in Figure 2: once a separator has been computed in parallel, by means of a method described below, each of the p processes participates in the building of the distributed induced subgraph corresponding to the first separated part (even if some processes do not have any vertex of it). This induced subgraph is then folded onto the first $\lceil \frac{p}{2} \rceil$ processes, such that the average number of vertices per process, which guarantees efficiency as it allows to overlap communications by a subsequent amount of computation, remains

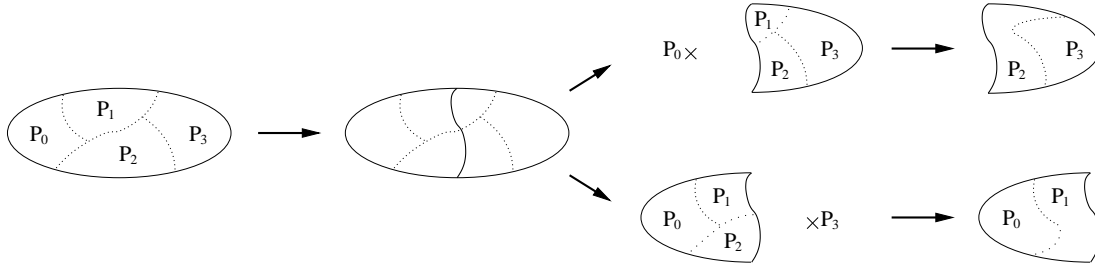


Figure 2. Diagram of a nested dissection step for a (sub-)graph distributed across four processes.

constant. During the folding phase, vertices and adjacency lists owned by the $\lfloor \frac{p}{2} \rfloor$ sender processes are redistributed across the $\lceil \frac{p}{2} \rceil$ receiver processes so as to evenly balance their loads.

The same procedure is used to build, on the $\lfloor \frac{p}{2} \rfloor$ remaining processes, the folded induced subgraph corresponding to the second part. These two constructions being completely independent, the computations of the two induced subgraphs and their folding can be performed in parallel, thanks to the temporary creation of an extra thread per process. When the vertices of the separated graph are evenly distributed across the processes, this feature favors load balancing in the subgraph building phase, because processes which do not have many of their vertices in one part have the rest of them in the other part, thus necessitating the same overall amount of work to create both graphs in the same time. This feature can be disabled when the communication system of the target machine is not thread-safe.

At the end of the folding phase, every process has a subgraph fragment of one of the two folded subgraphs, and the nested dissection algorithm can recursively proceed independently on each subgroup of $\frac{p}{2}$ (then $\frac{p}{4}$, $\frac{p}{8}$, etc.) processes, until each subgroup is reduced to a single process. From then on, the nested dissection algorithm will go on sequentially on every process, using the nested dissection routines of the SCOTCH library, eventually ending in a coupling with minimum degree methods [10] (which are thus only used in a sequential context).

3.2. Graph coarsening

The second level of concurrency concerns the computation of separators. The approach we have chosen is the now classical multi-level one [11–13]. It consists in repeatedly computing a set of increasingly coarser albeit topologically similar versions of the graph to separate, by finding matchings which collapse vertices and edges, until the coarsest graph obtained is no larger than a few hundreds of vertices, then computing a vertex separator on this coarsest graph, and projecting back this separator, from coarser to finer graphs, up to the original graph. Most often, a local optimization algorithm, such as Kernighan-Lin [14] or Fiduccia-Mattheyses [15] (FM), is used in the uncoarsening phase to refine the partition which is projected back at every level, such that the granularity of

the solution is the one of the original graph and not the one of the coarsest graph. Because we are interested in vertex separators, the refinement algorithm we use is a vertex-oriented variant of the FM algorithm, similar to the one described in [16].

The main features of our implementation are outlined in Figure 3. The matching of vertices is performed in parallel by means of a synchronous probabilistic algorithm. Every process works on a queue storing the yet unmatched vertices which it owns, and repeats the following steps. The queue head vertex is dequeued, and a candidate for mating is chosen among its unmatched neighbors, if any; else, the vertex is left unmatched at this level and discarded. When there are several unmatched neighbors, the candidate is randomly chosen among vertices linked by edges of heaviest weight, as in [17]. If the candidate vertex belongs to the same process, the mating is immediately recorded, else a mating request is stored in a query buffer to be sent to the proper neighbor process, and both vertices (the local vertex and its ghost neighbor) are flagged as temporarily unavailable. Once all vertices in queue have been considered, query buffers are exchanged between neighboring processes, and received query buffers are processed in order to satisfy feasible pending matings. Then, unsatisfied mating requests are notified to their originating processes, which unlock and reenqueue the unmatched vertices. This whole process is repeated until the list is almost empty; we do not wait until it is completely empty because it might require too many collective steps for just a few remaining vertices. It usually converges in 5 iterations.

The coarsening phase starts once the matching phase has converged. It can be parametrized so as to allow one to choose between two options. Either all coarsened vertices are kept on their local processes (that is, processes that hold at least one of the ends of the coarsened edges), as shown in the first steps of Figure 3, which decreases the number of vertices owned by every process and speeds-up future computations, or else coarsened graphs are folded and duplicated, as shown in the next steps of Figure 3, which increases the number of working copies of the graph and can thus reduce communication and improve the final quality of the separators. A folding algorithm is also implemented in *PARMETIS*, in the end of its multi-level process, to keep the number of vertices per process sufficiently high so as to prevent running time from being dominated by communications [18]. However, in its case, the folded subgraphs are not duplicated on the two subsets of processes, and its folding algorithm requires the number of sending processes to be even, such that the parallel graph ordering routine of *PARMETIS* can only work on a numbers of processes which are powers of two. *PT-SCOTCH* does not have this limitation, and can run on any number of processes.

As a matter of fact, separator computation algorithms, which are local heuristics, heavily depend on the quality of the coarsened graphs, and we have observed with the sequential version of *SCOTCH* that taking every time the best partition among two ones, obtained from two fully independent multi-level runs, usually improves overall ordering quality. By enabling the folding-with-duplication routine (which will be referred to as “fold-dup” in the following) in the first coarsening levels, one can implement this approach in parallel, every subgroup of processes that hold a working copy of the graph being able to perform an almost-complete independent multi-level computation, save for the very first level which is shared by all subgroups, for the second one which is shared by half of the subgroups, and so on.

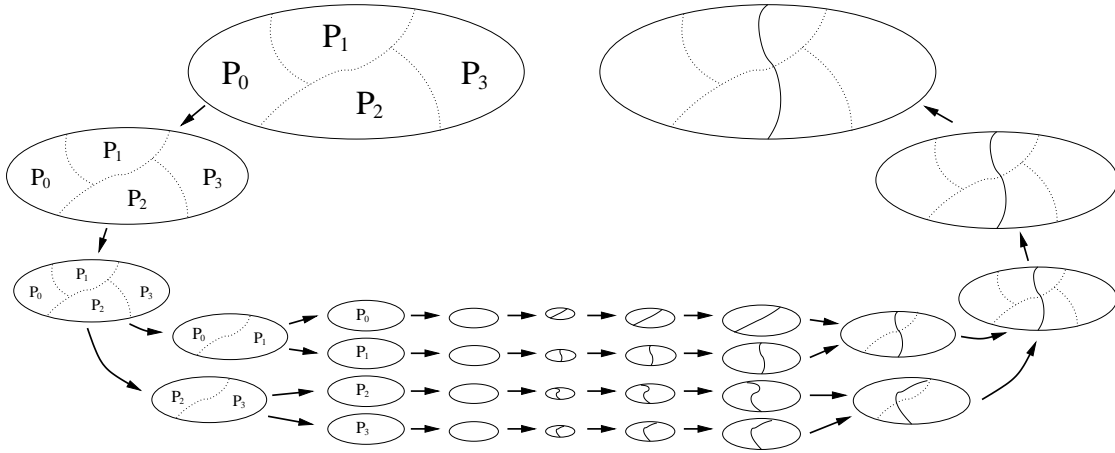


Figure 3. Diagram of the parallel computation of the separator of a graph distributed across four processes, by parallel coarsening with folding-with-duplication, multi-sequential computation of initial partitions that are locally projected back and refined on every process, and then parallel uncoarsening of the best partition encountered.

The problem with the fold-dup approach is that it consumes a lot of memory. When no folding occurs, and in the ideal case of a perfect and evenly balanced matching, the coarsening process yields on every process a part of the coarser graph which is half the size of the finer graph, and so on, such that the overall memory footprint on every process is about twice the size of the original graph. When folding occurs, every process receives two coarsened parts, one of which belonging to another process, such that the size of the folded part is about the one of the finer graph. The footprint of the fold-dup scheme is therefore logarithmic in the number of processes, and may consume all available memory as this number increases. Consequently, as in [19], a good strategy can be to resort to folding only when the number of vertices of the graph to be considered reaches some minimum threshold. This threshold allows one to set a trade-off between the level of completeness of the independent multi-level runs which result from the early stages of the fold-dup process, which impact partitioning quality, and the amount of memory to be used in the process.

Once all working copies of the coarsened graphs are folded on individual processes, the algorithm enters a multi-sequential phase, illustrated at the bottom of Figure 3: the routines of the sequential SCOTCH library are used on every process to complete the coarsening process, compute an initial partition, and project it back up to the largest centralized coarsened graph stored on each of the processes. Then, the partitions are projected back in parallel to the finer distributed graphs, selecting the best partition between the two available when projecting to a level where fold-dup had been performed. This distributed projection process is repeated until we obtain a partition of the original graph.

3.3. Band refinement

The third level of concurrency concerns the refinement heuristics which are used to improve the projected separators. At the coarsest levels of the multi-level algorithm, when computations are restricted to individual processes, the sequential vertex FM algorithm of SCOTCH is used, but this class of algorithms does not parallelize well. Indeed, a parallel FM-like algorithm has been proposed in PARMETIS [20] but, in order to relax the strong sequential constraint that would require some communication every time a vertex to be migrated has neighbors on other processes, only moves that strictly improve the partition are allowed, which hinders the ability of the FM algorithm to escape from local minima of its cost function, and leads to severe loss of partition quality when the number of processes (and thus of potential remote neighbors) increases.

This problem can be solved in two ways: either by developing scalable and efficient local optimization algorithms, or by being able to use the existing sequential FM algorithm on very large graphs. We have proposed and successfully tested in [21] a solution which enables both approaches, and is based on the following reasoning. Since every refinement is performed by means of a local algorithm, which perturbs only in a limited way the position of the projected separator, local refinement algorithms need only be passed a subgraph that contains the vertices that are very close to the projected separator. We have therefore implemented a distributed band graph extraction algorithm, which only keeps vertices that are at small distance from the projected separators, such that our local optimization algorithms are applied to these band graphs rather than to the whole graphs.

Using FM algorithms on band graphs substantially differs from what is called “boundary FM” in the literature [22,23]. This latter technique amounts in FM-like algorithms to recomputing gains of vertices which are in the immediate vicinity of the current separator only, in order to save computation time, and SCOTCH also benefits from this optimization, even on band graphs themselves. What differs with our use of band graphs is that feasible moves are limited to the band area, from which refined separators will never move away, while they could move far away from projected separators in the case of unconstrained FM, whether boundary-optimized or not.

We have experimented that, when performing FM refinement on band graphs that contain vertices that are at distance at most 3 from the projected separators, the quality of the finest separator does not only remain constant, but even improves in most cases, sometimes significantly. Our interpretation is that pre-constrained banding prevents local optimization algorithms from exploring and being trapped in local optima that would be too far from the global optimum sketched at the coarsest level of the multi-level process. The optimal band width value of 3 that we have evidenced is significant in this respect: it is the maximum distance at which two vertices can be in some graph when the coarse vertices to which they belong are neighbors in the coarser graph of next level. Therefore, keeping more layers of vertices in the band graph is not useful, because allowing the fine separator to move at a distance greater than 3 in the fine graph to reach some local optimum means that it could already have moved to this local optimum in the coarser graph, save for coarsening artefacts, which are indeed what we want not to be influenced by.

The advantage of pre-constrained band FM is that band graphs are of a much smaller

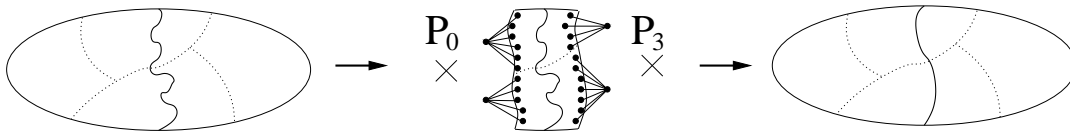


Figure 4. Creation of a distributed band graph from a projected partition. Once the separator of the band graph is refined, it is projected back to the original distributed graph.

size than their parent graphs, since for most graphs the size of the separators is of several orders of magnitude smaller than the size of the separated graphs: it is for instance in $O(n^{\frac{1}{2}})$ for 2D meshes, and in $O(n^{\frac{2}{3}})$ for 3D meshes [24]. Consequently, FM or other algorithms can be run on graphs that are much smaller, without decreasing separation quality.

The computation and use of distributed band graphs is outlined in Figure 4. Given a distributed graph and a projected separator, which can be spread across several processes, vertices that are closer to separator vertices than some small user-defined distance are selected by spreading distance information from all of the separator vertices, using our halo exchange routine. Then, the distributed band graph is created, by adding on every process two anchor vertices, which are connected to the last layers of vertices of each of the parts. The vertex weight of the anchor vertices is equal to the sum of the vertex weights of all of the vertices they replace, to preserve the balance of the two band parts. Once the separator of the band graph has been refined using some local optimization algorithm, the new separator is projected back to the original distributed graph.

Basing on our band graphs, we have implemented a multi-sequential refinement algorithm, outlined in Figure 5. At every distributed uncoarsening step, a distributed band graph is created. Centralized copies of this band graph are then gathered on every participating process, which serve to run fully independent instances of our sequential FM algorithm. The perturbation of the initial state of the sequential FM algorithm on every process allows us to explore slightly different solution spaces, and thus to improve refinement quality. Finally, the best refined band separator is projected back to the distributed graph, and the uncoarsening process goes on.

Centralizing band graphs is an acceptable solution because of the much reduced size of the band graphs that are centralized on the processes. Using this technique, we expect to achieve our goal, that is, to be able partition graphs up to a billion vertices, distributed on a thousand processes, without significant loss in quality, because centralized band graphs will be of a size of a few million vertices for 3D meshes. In case the band graph cannot be centralized, we can resort to a fully scalable algorithm, as partial copies can also be used collectively to run a scalable parallel multi-deme genetic optimization algorithm, such as the one experimented with in [21].

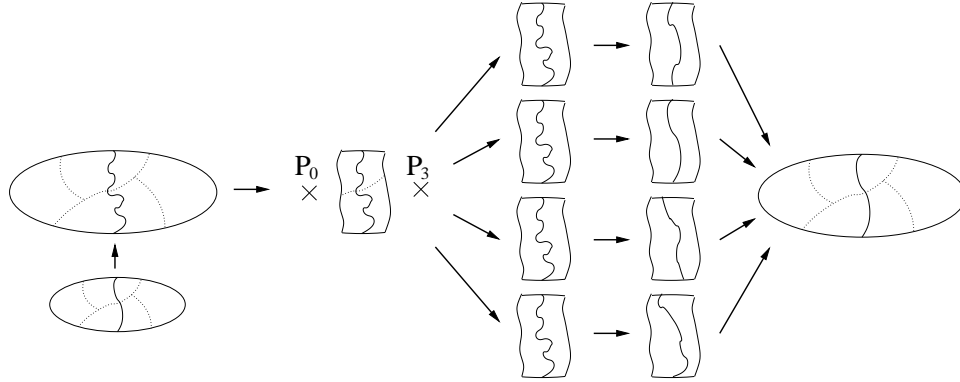


Figure 5. Diagram of the multi-sequential refinement of a separator projected back from a coarser graph distributed across four processes to its finer distributed graph.

4. Experimental results

PT-SCOTCH is written in ANSI C, with calls to the POSIX thread and MPI APIs. The largest test graphs that we have used to date in our experiments are presented in Table 1. All of our tests were performed on the M3PEC system of Université Bordeaux 1, an IBM cluster of SMP nodes made of 8 dual-core Power5 processors running at 1.5 GHz.

All of the ordering strategies that we have used were based on the multi-level scheme. During the uncoarsening step, separator refinement was performed by using our sequential FM algorithm on band graphs of width 3 around the projected separators, both in the parallel (with multi-centralized copies) and in the sequential phases of the uncoarsening process.

The quality of orderings is evaluated with respect to two criteria. The first one, NNZ (“number of non-zeros”), is the number of non-zero terms in the factored reordered matrix, which can be divided by the number of non-zero terms in the initial matrix to give the fill ratio of the ordering. The second one, OPC (“operation count”), is the number of arithmetic operations required to factor the matrix using the Cholesky method. It is equal to $\sum_c n_c^2$, where n_c is the number of non-zeros of column c of the factored matrix, diagonal included.

For the sake of reproducibility, the random generator used in SCOTCH is initialized with a fixed seed. This feature is essential to end users, who can more easily reproduce their experiments and debug their own software, and is not significant in term of performance. Indeed, on 64 processors, we have experimented that the maximum variation of ordering quality, in term of OPC, between 10 runs performed with varying random seed, was less than 2.2 percent on all of the above test graphs, while running time was not impacted. Consequently, it is not necessary for us to perform multiple runs of SCOTCH to average quality measures.

Tables 2 and 3 present the OPC computed on the orderings yielded by PT-SCOTCH and PARMETIS. These results have been obtained by running PT-SCOTCH with the

Graph	Size ($\times 10^3$)		Average degree	O_{SS}	Description
	$ V $	$ E $			
23millions	23114	175686	7.60	1.29e+14	3D electromagnetics, CEA
altr4	26	163	12.50	3.65e+8	3D electromagnetics, CEA
audikw1	944	38354	81.28	5.48e+12	3D mechanics mesh, Parasol
bmw32	227	5531	48.65	2.80e+10	3D mechanics mesh, Parasol
brgm	3699	151940	82.14	2.70e+13	3D geophysics mesh, BRGM
cake15	5154	47022	18.24	4.06e+16	DNA electrophoresis, UF
conesphere1m	1055	8023	15.21	1.83e+12	3D electromagnetics, CEA
coupole8000	1768	41657	47.12	7.46e+10	3D structural mechanics, CEA
qimonda07	8613	29143	6.76	8.92e+10	Circuit simulation, Qimonda
thread	30	2220	149.32	4.14e+10	Connector problem, Parasol

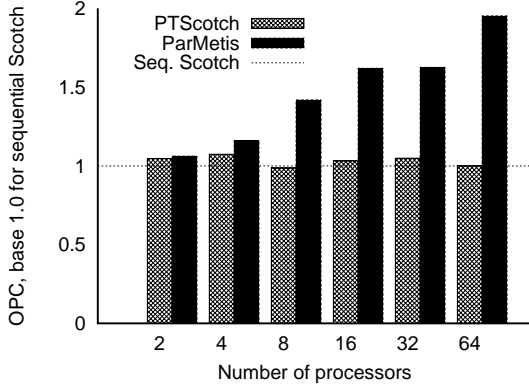
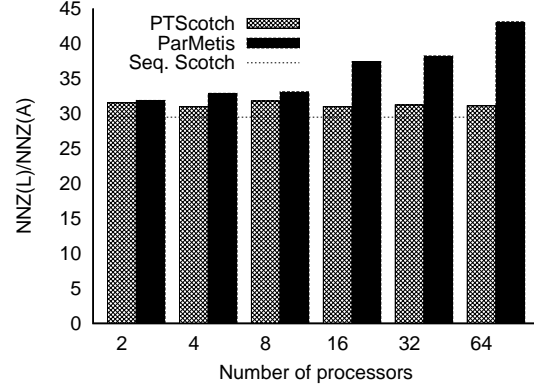
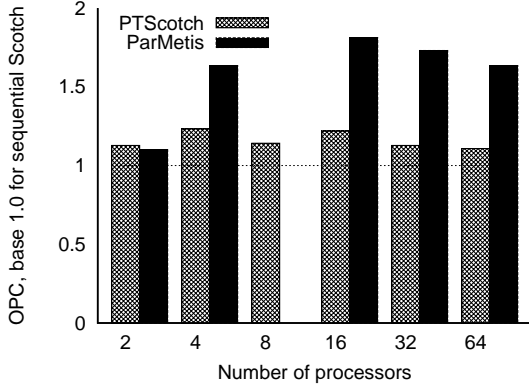
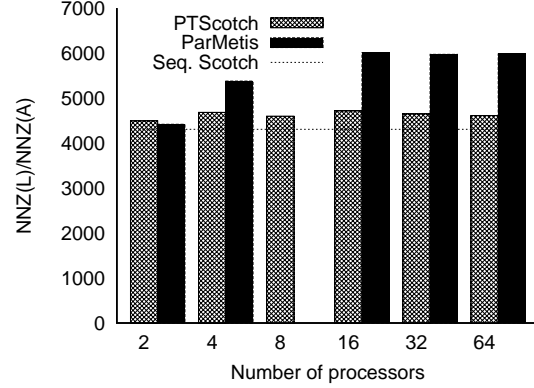
Table 1

Description of some of the test graphs that we use. $|V|$ and $|E|$ are the vertex and edge cardinalities, in thousands, and O_{SS} is the operation count of the Cholesky factorization performed on orderings computed using the sequential SCOTCH software. CEA is the French atomic energy agency, UF stands for the University of Florida sparse matrix collection [25], and Parasol is a former European project [26].

following default strategy: in the multi-level process, graphs are coarsened without any folding until the average number of vertices per process becomes smaller than 100, after which the fold-dup process takes place until all graphs are folded on single processes and the sequential multi-level process relays it.

The improvement in quality brought by PT-SCOTCH is clearly evidenced. Ordering quality does not decrease along with the number of processes, as our local optimization scheme is not sensitive to it, but instead most often slightly increases, because of the increased number of multi-sequential optimization steps which can be run in parallel. Graphics in Figures 6 to 9 evidence that PT-SCOTCH clearly outperforms PARMETIS in term of ordering quality. For both graphs, the results of PT-SCOTCH are very close to the ones obtained by the sequential SCOTCH software, while the costs of PARMETIS orderings increase dramatically along with the number of processes.

While PT-SCOTCH is, at the time being, about four times slower on average than PARMETIS, it can yield operation counts that are as much as two times smaller than the ones of this latter, which is of interest as factorization times are more than one order of magnitude higher than ordering times. For example, it takes only 41 seconds to PT-SCOTCH to order the **brgm** matrix on 64 processes, and about 280 seconds to MUMPS [27] to factorize the reordered matrix on the same number of processes. As the factorization process is often very scalable, it can happen, for very large numbers of processes, that ordering times with PT-SCOTCH are higher than factorization times, because communication latencies dominate and scalability can no longer be guaranteed. Because of their different complexity and scalability behaviors, it is in general not useful to run the ordering tool on as many processes as the solver; what matters is to have enough distributed memory to store the graph and run the ordering process, while keeping good

Figure 6. OPC for graph **audikw1**.Figure 7. NNZ fill ratio for graph **audikw1**.Figure 8. OPC for graph **cage15**.Figure 9. NNZ fill ratio for graph **cage15**.

scalability in time. Moreover, in various applications, the ordering phase is performed only once while the factorization step is repeated many times with different numerical values, the matrix structure being invariant. This is the reason why we essentially focused on ordering quality rather than on optimal scalability.

The multi-sequential FM refinement algorithm that we use is by nature not scalable, and its cost, even on band graphs, is bound to dominate parallel execution time when the number of processors increases. This is why on some graphs, depending on their size, average degree and topology, running times of PT-SCOTCH no longer decrease. We are therefore still working on improving the scalability in time of PT-SCOTCH, and especially of its coarsening phase, which is the most time-consuming algorithm in term of communications. We are also investigating several ways to replace the intrinsically sequential FM refinement algorithm by fully parallel algorithms such as parallel diffusion-based methods [28] or genetic algorithms [21].

Figures 10 and 11 show the amount of memory used per process during the ordering of two of our test graphs. Figure 10 evidences that, despite the use of folding and duplication at the coarsest levels, memory scalability remains good. However, imbalance can be high, especially for graph **audikw1**. Because this graph possesses a set of contiguous vertices

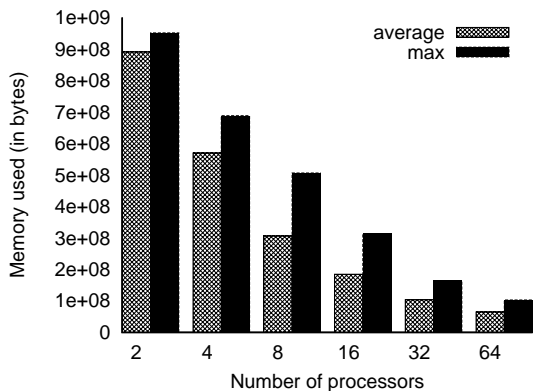


Figure 10. Memory used per process to reorder graph **audikw1**.

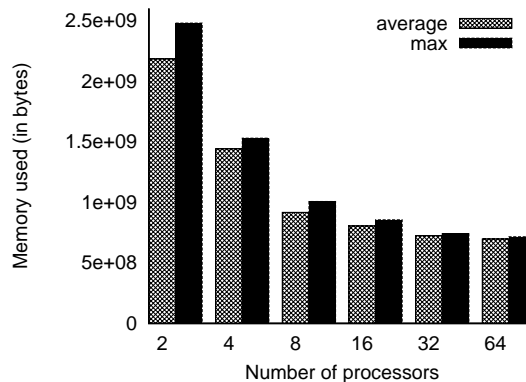


Figure 11. Memory used per process to reorder graph **cage15**.

of very high degree, and as all of our data distributions balance numbers of vertices only, there can be cases in which one process holds most of the edges by owning entirely the subset of highly connected vertices. Also, for graph **cage15**, memory scalability can only be observed between two and eight processes. The main reason is that the vertices of this graph are initially ordered such that the number of ghost vertices quickly increases when the number of processes reaches 16. However, since this graph is of low degree, memory scalability will eventually be evidenced again, in term of edges rather than of vertices, after all edges are considered to be connected to ghost vertices.

5. Conclusion

We have presented in this paper the parallel algorithms that we have implemented in PT-SCOTCH to compute in parallel efficient orderings of very large graphs. The first results are encouraging, as they meet the expected performance requirements in term of quality, but have yet to be improved in term of scalability. Indeed, scalability can only be partially evidenced for very large graphs, because of the lack of scalability of our multi-sequential band refinement algorithm. However, we have been able to run test graphs which could not fit in memory when processed by competing software.

To date, we have been able to order 3D graphs up to 23 million vertices, which have been successfully factorized afterwards, in double precision complex arithmetic, by the PASTIX parallel direct solver [29] also developed within the SCALAPPLIX project. Although existing parallel direct sparse linear system solvers cannot currently handle full 3D meshes of sizes larger than about fifty million unknowns, we plan to use PT-SCOTCH to compute orderings of larger matrices to be factorized using hybrid direct-iterative schemes [30,31].

However, sparse matrix ordering is not the application field in which we expect to find the largest problem graphs. Basing on the software building blocks that we have already written, we plan to extend the capabilities of PT-SCOTCH to compute edge-separated k-ary partitions of large meshes for subdomain-based fully iterative methods, as well as static mappings of process graphs, like the SCOTCH library does sequentially.

REFERENCES

1. METIS: Family of multilevel partitioning algorithms, <http://glaros.dtc.umn.edu/gkhome/views/metis>.
2. JOSTLE: Graph partitioning software, <http://staffweb.cms.gre.ac.uk/~c.walshaw/jostle/>.
3. SCOTCH: Static mapping, graph partitioning, and sparse matrix block ordering package, <http://www.labri.fr/~pelegrin/scotch/>.
4. W. F. Tinney, J. W. Walker, Direct solutions of sparse network equations by optimally ordered triangular factorization, *J. Proc. IEEE* 55 (1967) 1801–1809.
5. P. Amestoy, T. Davis, I. Duff, An approximate minimum degree ordering algorithm, *SIAM J. Matrix Anal. and Appl.* 17 (1996) 886–905.
6. A. George, J. W.-H. Liu, The evolution of the minimum degree ordering algorithm, *SIAM Review* 31 (1989) 1–19.
7. J. W.-H. Liu, Modification of the minimum-degree algorithm by multiple elimination, *ACM Trans. Math. Software* 11 (2) (1985) 141–153.
8. T.-Y. Chen, J. R. Gilbert, S. Toledo, Toward an efficient column minimum degree code for symmetric multiprocessors, in: *Proc. 9th SIAM Conf. on Parallel Processing for Scientific Computing*, San-Antonio, 1999.
9. J. A. George, J. W.-H. Liu, *Computer solution of large sparse positive definite systems*, Prentice Hall, 1981.
10. F. Pellegrini, J. Roman, P. Amestoy, Hybridizing nested dissection and halo approximate minimum degree for efficient sparse matrix ordering, *Concurrency: Practice and Experience* 12 (2000) 69–84.
11. S. T. Barnard, H. D. Simon, A fast multilevel implementation of recursive spectral bisection for partitioning unstructured problems, *Concurrency: Practice and Experience* 6 (2) (1994) 101–117.
12. B. Hendrickson, R. Leland, A multilevel algorithm for partitioning graphs, in: *Proceedings of Supercomputing*, 1995.
13. G. Karypis, V. Kumar, A fast and high quality multilevel scheme for partitioning irregular graphs, *SIAM Journal on Scientific Computing* 20 (1) (1998) 359–392.
14. B. W. Kernighan, S. Lin, An efficient heuristic procedure for partitioning graphs, *BELL System Technical Journal* (1970) 291–307.
15. C. M. Fiduccia, R. M. Mattheyses, A linear-time heuristic for improving network partitions, in: *Proc. 19th Design Automation Conference, IEEE*, 1982, pp. 175–181.
16. B. Hendrickson, E. Rothberg, Improving the runtime and quality of nested dissection ordering, *SIAM Journal of Scientific Computing* 20 (2) (1998) 468–489.
17. G. Karypis, V. Kumar, A fast and high quality multilevel scheme for partitioning irregular graphs, *Tech. Rep. 95-035*, University of Minnesota (Jun. 1995).
18. G. Karypis, V. Kumar, A coarse-grain parallel formulation of multilevel k -way graph-partitioning algorithm, in: *Proc. 8th SIAM Conference on Parallel Processing for Scientific Computing*, 1997.
19. G. Karypis, V. Kumar, *PARMETIS: Parallel Graph Partitioning and Sparse Matrix Ordering Library*, University of Minnesota (Aug. 2003).
20. G. Karypis, V. Kumar, Parallel multilevel k -way partitioning scheme for irregular

- graphs, Tech. Rep. 96-036, University of Minnesota (May 1996).
21. C. Chevalier, F. Pellegrini, Improvement of the efficiency of genetic algorithms for scalable parallel graph partitioning in a multi-level framework, in: Proc. EuroPar, Dresden, LNCS 4128, 2006, pp. 243–252.
 22. B. Hendrickson, R. Leland, The CHACO user’s guide, Tech. Rep. SAND93–2339, Sandia National Laboratories (Nov. 1993).
 23. G. Karypis, V. Kumar, METIS - A Software Package for Partitioning Unstructured Graphs, Partitioning Meshes, and Computing Fill-Reducing Orderings of Sparse Matrices, University of Minnesota, 4th Edition (Sep. 1998).
 24. R. J. Lipton, D. J. Rose, R. E. Tarjan, Generalized nested dissection, SIAM Journal of Numerical Analysis 16 (2) (1979) 346–358.
 25. T. Davis, University of Florida Sparse Matrix Collection, <http://www.cise.ufl.edu/research/sparse/matrices/>.
 26. PARASOL project (EU ESPRIT IV LTR Project No. 20160) (1996–1999).
 27. P. Amestoy, I. Duff, J.-Y. L’Excellent, Multifrontal parallel distributed symmetric and unsymmetric solvers, Computer methods in applied mechanics and engineering. 184 (2000) 501–520, special issue on Domain Decomposition and Parallel Computing.
 28. F. Pellegrini, A parallelisable multi-level banded diffusion scheme for computing balanced partitions with smooth boundaries, in: Proc. Euro-Par, Rennes, Vol. 4641 of LNCS, 2007, pp. 191–200, http://www.labri.fr/~pelegri/papers/scotch-bipart_diffusion_europar2007.pdf.
 29. P. Hénon, P. Ramet, J. Roman, On using an hybrid MPI-Thread programming for the implementation of a parallel sparse direct solver on a network of SMP nodes, in: Proceedings of Sixth International Conference on Parallel Processing and Applied Mathematics, Poznan, Poland, 2005.
 30. P. Hénon, Y. Saad, A parallel multistage ILU factorization based on a hierarchical graph decomposition, SIAM Journal of Scientific Computing 28 (2006) 2266–2293.
 31. P. Hénon, P. Ramet, J. Roman, On finding approximate supernodes for an efficient block $ILU(k)$ factorization, Parallel Computing To appear.

Test case	Number of processes					
	2	4	8	16	32	64
23millions						
O_{PTS}	1.45e+14	2.91e+14	3.99e+14	2.71e+14	1.94e+14	2.45e+14
O_{PM}	†	†	†	†	†	†
t_{PTS}	671.60	416.75	295.38	211.68	147.35	103.73
t_{PM}	†	†	†	†	†	†
altr4						
O_{PTS}	3.84e+8	3.75e+8	3.93e+8	3.69e+8	4.09e+8	4.15e+8
O_{PM}	4.20e+8	4.49e+8	4.46e+8	4.64e+8	5.03e+8	5.16e+8
t_{PTS}	0.42	0.30	0.24	0.30	0.52	1.55
t_{PM}	0.31	0.20	0.13	0.11	0.13	0.33
audikw1						
O_{PTS}	5.73e+12	5.65e+12	5.54e+12	5.45e+12	5.45e+12	5.45e+12
O_{PM}	5.82e+12	6.37e+12	7.78e+12	8.88e+12	8.91e+12	1.07e+13
t_{PTS}	73.11	53.19	45.19	33.83	24.74	18.16
t_{PM}	32.69	23.09	17.15	9.804	5.65	3.82
bmw32						
O_{PTS}	3.50e+10	3.49e+10	3.14e+10	3.05e+10	3.02e+10	3.00e+10
O_{PM}	3.22e+10	4.09e+10	5.11e+10	5.61e+10	5.74e+10	6.31e+10
t_{PTS}	8.89	7.41	5.68	5.45	8.36	17.64
t_{PM}	3.39	2.28	1.51	0.92	0.68	1.08
brgm						
O_{PTS}	2.70e+13	2.55e+13	2.65e+13	2.88e+13	2.86e+13	2.87e+13
O_{PM}	–	†	†	†	†	†
t_{PTS}	276.9	167.26	97.69	61.65	42.85	41.00
t_{PM}	–	†	†	†	†	†
cage15						
O_{PTS}	4.58e+16	5.01e+16	4.64e+16	4.95e+16	4.58e+16	4.50e+16
O_{PM}	4.47e+16	6.64e+16	†	7.36e+16	7.03e+16	6.64e+16
t_{PTS}	540.46	427.38	371.70	340.78	351.38	380.69
t_{PM}	195.93	117.77	†	40.30	22.56	17.83
conesphere1m						
O_{PTS}	1.88e+12	1.89e+12	1.85e+12	1.84e+12	1.86e+12	1.77e+12
O_{PM}	2.20e+12	2.46e+12	2.78e+12	2.96e+12	2.99e+12	3.29e+12
t_{PTS}	31.34	20.41	18.76	18.37	25.80	92.47
t_{PM}	22.40	11.98	6.75	3.89	2.28	1.87

Table 2

Comparison between PT-SCOTCH (PTS) and PARMETIS (PM) for several graphs. O_{PTS} and O_{PM} are the OPC for PTS and PM, respectively. Dashes indicate abortion due to memory shortage. Daggers indicate abortion due to an invalid MPI operation.

Test case	Number of processes					
	2	4	8	16	32	64
coupole8000						
O_{PTS}	8.68e+10	8.54e+10	8.38e+10	8.03e+10	8.26e+10	8.21e+10
O_{PM}	†	†	8.17e+10	8.26e+10	8.58e+10	8.71e+10
t_{PTS}	114.41	116.83	85.80	60.23	41.60	28.10
t_{PM}	63.44	37.50	20.01	10.81	5.88	3.14
qimonda07						
O_{PTS}	–	–	5.80e+10	6.38e+10	6.94e+10	7.70e+10
O_{PM}	†	†	†	†	†	†
t_{PTS}	–	–	34.68	22.23	17.30	16.62
t_{PM}	†	†	†	†	†	†
thread						
O_{PTS}	3.52e+10	4.31e+10	4.13e+10	4.06e+10	4.06e+10	4.50e+10
O_{PM}	3.98e+10	6.60e+10	1.03e+11	1.24e+11	1.53e+11	–
t_{PTS}	3.66	3.61	3.30	3.65	5.68	11.16
t_{PM}	1.25	1.05	0.68	0.51	0.40	–

Table 3
Continuation of Table 2.